



Syngas Production Through H₂O/CO₂ Thermochemical Splitting Over Doped Ceria-Zirconia Materials

Giuseppina Luciani¹, Gianluca Landi^{2*} and Almerinda Di Benedetto¹

¹ Dipartimento di Ingegneria Chimica, dei Materiali e della Produzione Industriale, Università di Napoli Federico II, Naples, Italy, ² Istituto di Ricerche sulla Combustione – CNR, Naples, Italy

This study investigates the catalytic properties of K⁺ and Cu²⁺/Fe³⁺ co-doped ceria-zirconia (CeZr) toward water and carbon dioxide co-splitting. These materials can convert separate feeds of CO₂ and H₂O into CO and H₂. In co-splitting tests, water reacts faster on the K-Cu-CeZr catalyst with negligible CO production. The reduction of the K-Fe-CeZr catalyst occurs over two broad temperature ranges: at low temperature, only H₂ is produced; whereas CO is the most abundant product at high temperature. A kinetic model was developed to get insights into the reasons of the observed selectivity toward H₂ at low temperature and CO at a higher temperature. The different reaction orders in the sites fraction were evaluated for CO₂ and H₂O reactions, highlighting that H₂ production requires a larger number of adjacent reduced sites than CO production. Three regimes were identified through the model: Regime I- H₂O driven regime @T ≤ 650°C; Regime II- mixed regime @ 560 < T < 700°C and Regime III: CO₂ driven regime @ T > 700°C. These results indicate the appropriate conditions for tuning H₂/CO selectivity, depending on the feed composition.

Keywords: thermochemical water splitting, thermochemical CO₂ splitting, sustainable energy, transition metals, potassium, ceria-zirconia, kinetic modeling

OPEN ACCESS

Edited by:

Alfonso Chinnici,
University of Adelaide, Australia

Reviewed by:

Mahyar Silakhori,
University of Adelaide, Australia
Gang Liu,
Central South University, China

*Correspondence:

Gianluca Landi
gianluca.land@cnr.it

Specialty section:

This article was submitted to
Process and Energy Systems
Engineering,
a section of the journal
Frontiers in Energy Research

Received: 26 May 2020

Accepted: 31 July 2020

Published: 05 October 2020

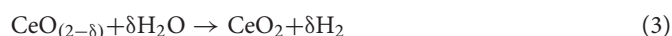
Citation:

Luciani G, Landi G and
Di Benedetto A (2020) Syngas
Production Through H₂O/CO₂
Thermochemical Splitting Over Doped
Ceria-Zirconia Materials.
Front. Energy Res. 8:204.
doi: 10.3389/fenrg.2020.00204

INTRODUCTION

The transformation of solar energy into synthetic fuels holds huge promise for sustainable approaches to harvesting renewable energy (Nguyen and Blum, 2015; Chuayboon and Abanades, 2020; Mao et al., 2020). Thermochemical splitting cycles have been proposed as a promising sustainable option, as this approach uses concentrated solar energy to convert H₂O and CO₂ into H₂ and CO (Costa Oliveira et al., 2018; Bhosale et al., 2019; Takalkar et al., 2019). These building blocks can be further reacted into gaseous and liquid fuels.

Among thermochemical cycles, two-step high temperature processes are the most promising (Rao and Dey, 2015), because they are less complex and can achieve a higher and more efficient theoretical solar-to-fuel energy conversion ($\eta_{solar-to-fuel}$) (Rao and Dey, 2015). The thermochemical splitting catalyst ceria is recognized as an important development (Bhosale et al., 2019) due to its thermal stability, high oxygen storage capacity (OSC), without any structural changes, and the fast kinetics of reduction and splitting reactions (Costa Oliveira et al., 2018; Bhosale et al., 2019; Chen et al., 2019; Takalkar et al., 2019). The thermochemical cycle can be schematically defined as follows:



Reaction 1 corresponds to high temperature self-reduction under concentrated solar power, whereas reactions 2 and 3 are the splitting reactions, which restore the oxidized state of the materials and producing fuels.

Despite the huge CeO₂ potential in thermochemical cycles, high reduction temperature (step1), compromising long-term thermal stability over multiple cycles as well as small fuel production still limits its technological application. To date, a number of other studies have addressed these issues (Kaneko et al., 2011; Petkovich et al., 2011; Gokon et al., 2013, 2015a; Agrafiotis et al., 2015; Jarrett et al., 2016; Muhich et al., 2016; Al-Shankiti et al., 2017; Cho et al., 2017; Zhou et al., 2017; Luciani et al., 2019; Bhosale and AlMomani, 2020; Costa Oliveira et al., 2020; Haeussler et al., 2020). Modifying ceria fluorite structure with metal cations has proved to be a successful strategy for improving both oxygen ion mobility and thermal stability, ultimately enhancing the redox activity of the material (Kang et al., 2013; Cooper et al., 2015; Gokon et al., 2015a,b; Takacs et al., 2015; Bhosale et al., 2016; Lin et al., 2016; Zhao et al., 2016; Mostrou et al., 2017; Muhich and Steinfeld, 2017; Bhosale and Takalkar, 2018; Takalkar et al., 2018, 2020a,b; Naghavi et al., 2020).

It is widely accepted that ceria-zirconia solid solutions, in particular those with a Ce/Zr molar ratio ~ 3 , show improved splitting properties, especially in terms of self-reducibility (Abanades et al., 2010; Kaneko et al., 2011; Le Gal and Abanades, 2011; Abanades and Le Gal, 2012; Call et al., 2013; Le Gal et al., 2013; Jacot et al., 2017; Muhich and Steinfeld, 2017). Moreover, the performance of this class of materials can be further enhanced by doping with bi- or trivalent cations, such as Cu²⁺, Mn³⁺, Fe³⁺ (Gokon et al., 2015a,b; Lin et al., 2016).

The improved splitting activity of ceria-zirconia solid solutions has been related to the formation of a Zr₂ON₂ like-phase at the nanoscale level during thermal treatment in N₂ atmosphere (Pappacena et al., 2016, 2017), which is associated with a decrease of surface Ce/Zr ratio (Luciani et al., 2019). Good splitting performance has been related also to the formation of both bulk and surface oxygen vacancies, enhancing surface reactivity (oxygen evolution during self-reduction and splitting reactivity during oxidation) and oxygen diffusivity from the bulk to the surface and vice-versa (Luciani et al., 2019).

While a huge amount of literature has been devoted to the thermochemical splitting of bare H₂O or CO₂, little is known about their simultaneous splitting (Furler et al., 2012; Lorentzou et al., 2014, 2017; Falter and Pitz-Paal, 2018; de la Calle and Bayon, 2019; Tou et al., 2019; Hao et al., 2020). It is worth noting that *co-splitting* has been generally defined as *concurrent* or *combined* splitting, but it should be better defined as *competitive* splitting; as a matter of fact, CO₂ and H₂O compete for the same reduced sites, whereas the overall fuel production depends on the reduction extent of the material.

Recently, we proved that potassium cation doping improved Ce_{0.75}Zr_{0.25}O₂ splitting performance toward CO₂ or H₂O (Landi, 2019). Alkali metal ions doping as well as transition metals cations co-doping, such as Cu(II) and Fe(III), provided the formation of both bulk and surface oxygen vacancies, significantly enhancing the splitting performance. Interestingly,

K-addition boosted the oxidation kinetics, in agreement with the results obtained in the three step cycles (Charvin et al., 2009). Recently, Takalkar et al. showed a positive effect of Li⁺ cation on the CO production during CO₂ splitting cycles (Takalkar et al., 2020b).

In this work, K-M-doped ceria-zirconia solid solutions (M = Cu²⁺ and Fe³⁺), containing 5% mol/mol of both K and M cations, were tested as catalysts for carbon dioxide and water co-splitting. Furthermore, a kinetic model was developed and used to get insights into the active sites of the catalysts and their activity toward H₂O and CO₂ splitting, to simulate the splitting performance as well as the composition of produced gases at different oxidation temperatures.

MATERIALS AND METHODS

Materials Preparation

Reagents were purchased from Sigma-Aldrich and used as received. The material synthesis was carried out by employing the following reagents: cerium (III) nitrate hexahydrate, Ce(NO₃)₃·6H₂O; zirconium (IV) oxynitrate hydrate, ZrO(NO₃)₂·xH₂O; iron (III) nitrate non ahydrate, Fe(NO₃)₃·9H₂O; potassium nitrate, KNO₃; copper (II) nitrate tetrahydrate, Cu(NO₃)₂·4H₂O; and manganese (II) nitrate tetrahydrate, Mn(NO₃)₂·4H₂O. The Ce/Zr molar ratio was kept constant at 3 (Ce_{0.75}Zr_{0.25}O₂ as general formula) since it ensured the highest reducible performance among CeO₂-ZrO₂ solutions (Le Gal and Abanades, 2012).

Bare ceria-zirconia, as well as doped and co-doped materials, were prepared according to the co-precipitation method (Luciani et al., 2018; Landi, 2019). Stoichiometric amounts of precursor salts were dissolved in 75 ml of bi-distilled water and stirred for 3 h. Then, solutions were heated in an MW oven (CEM SAM-155) until a homogeneous gel was obtained. The calcination in air at 1,100°C for 4 h was then carried out to decompose nitrates and to obtain the oxides. **Table 1** summarizes the composition of produced materials as well as the label used.

H₂O/CO₂ Splitting and Co-splitting Tests

The experimental equipment and experimental details described above were used to assess the splitting ability of the samples under investigation (Luciani et al., 2018, 2019; Portarapillo et al., 2019). Temperature programmed reduction (TPR) and oxidation (TPO) were carried out on powdered samples (500 mg; 170–300 μm), placed in a tubular quartz reactor, and inserted into an electric tubular furnace (Lenton). The catalyst temperature was measured by a K-type thermocouple placed inside a tube co-axial with the reactor.

As previously reported (Luciani et al., 2018, 2019; Portarapillo et al., 2019), the samples were pre-treated in a hydrogen flow (TPR; 10 l(SLT)/h; 5 vol.% H₂/N₂) up to approximately 1,000°C, heating rate 10°C/min (Al-Shankiti et al., 2013; Pappacena et al., 2016, 2017) and cooled down to 60°C under a nitrogen flow. TPO was then carried out by flowing (i) a 3 vol.% H₂O/N₂ mixture (10 l(SLT)/h), (ii) a 6 vol.% CO₂/N₂ mixture (10 l(SLT)/h), (iii) a (6 vol.% H₂O + 6 vol.% CO₂)/N₂ mixture (10 l(SLT)/h); the

temperature raised up to about 1,000°C (heating rate: 10°C/min; time at the maximum temperature: 20 min). We chose to use a diluted mixture according to the method outlined by Petkovich et al. (2011), to avoid a fast reaction, especially on H₂-reduced samples. The consistency of this approach has been demonstrated (Luciani et al., 2018, 2019; Portarapillo et al., 2019). The reduction and oxidation profiles were deconvoluted using OriginPro 8.5 software.

Oxygen, hydrogen, and carbon monoxide amounts (mol/g), n_{O_2} , n_{H_2} , and n_{CO} respectively, were calculated as follows:

$$n_{O_2,i} = \frac{2 \cdot n_{H_2_cons,i}}{m_{cat}} = \frac{2 \cdot \frac{area_{H_2_cons,i}}{100} \cdot F_{red} \cdot \frac{P}{R \cdot T}}{m_{cat}} \quad (4)$$

$$n_{H_2,i} = \frac{n_{H_2_prod,i}}{m_{cat}} = \frac{\frac{area_{H_2_prod,i}}{100} \cdot F_{ox} \cdot \frac{P}{R \cdot T}}{m_{cat}} \quad (5)$$

$$n_{CO,i} = \frac{n_{CO_prod,i}}{m_{cat}} = \frac{\frac{area_{CO_prod,i}}{100} \cdot F_{ox} \cdot \frac{P}{R \cdot T}}{m_{cat}} \quad (6)$$

where m_{cat} (g) is the sample mass, P (atm) and T (K) are standard pressure and temperature, R (atm·l·mol⁻¹·K⁻¹) is the ideal gas constant, F_{red} and F_{ox} (l(STP)/s) are the flow rates of permanent gases during H₂ treatment and splitting test, respectively, $n_{H_2_cons,i}$ and $n_{H_2_prod,i}$ are consumed and produced hydrogen moles during the H₂ reduction treatment and splitting test, respectively. The $area_{H_2_cons,i}$ and $area_{H_2_prod,i}$ (%·s) are the calculated areas of the reduction and oxidation H₂ profiles, respectively. $n_{CO_prod,i}$ is the amount of carbon monoxide produced during the splitting test, and $area_{CO_prod,i}$ (%·s) is the calculated area of the oxidation CO profile. The n_{O_2} does not represent a real molecular oxygen evolution but oxygen subtracted from the materials.

The reduction degree ($x_{red,i}$) after the current reduction or oxidation step (i) was calculated as follows:

$$x_{red,i} = x_{red,i-1} + \frac{n_{O_2,i}}{n_{O_2,max}} \quad (7a)$$

and as in the following for oxidation steps:

$$x_{red,i} = x_{red,i-1} - \frac{n_{H_2,i}}{2 \cdot n_{O_2,max}} \quad (7b)$$

$$x_{red,i} = x_{red,i-1} - \frac{n_{CO,i}}{2 \cdot n_{O_2,max}} \quad (7c)$$

where $n_{O_2,max}$ is the maximum O₂ amount (mol/g) that could be evolved, if reducible cations were reduced to their lowest oxidation state (Ce⁴⁺ to Ce³⁺, Fe³⁺ to Fe²⁺, Cu²⁺ to Cu⁰); corresponding values are reported in **Table 1**. $x_{red,i-1}$ is the

reduction degree of the previous (oxidation or reduction) step. Therefore, $x_{red,i}$ does not simply quantify the current fraction of Ce³⁺ ions on the overall content of Ce atoms in the system.

Oxidation yield (α_i) is calculated through produced CO (mol/g) during the current re-oxidation step and the corresponding O₂ evolved amount (mol/g) during the previous reduction step:

$$\alpha_i = \frac{n_{CO,i}}{2 \cdot n_{O_2,i-1}} \quad (8)$$

Reduction yield (β_i) is calculated through the overall O₂ amount (mol/g) produced during the current reduction step and CO evolved amount (mol/g) during the previous oxidation step:

$$\beta_i = \frac{2 \cdot n_{O_2,i}}{n_{CO,i-1}} \quad (9)$$

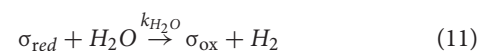
Kinetic Model

A kinetic model was developed to get insights into the role of the superficial reaction on the selectivity in co-fed splitting.

The model is based on the Polanyi-Wigner equation under the Redhead approximation, which states that catalytic sites do not interact. The reactor is modeled as a continuous stirred tank reactor (CSTR).

The reaction mechanism is a redox pathway involving active sites σ : σ_{red} as the reduced form and σ_{ox} as the oxidized form.

According to these hypotheses, the reaction steps are:



Sites fractions are defined by the following equations:

$$\theta_{red} = \frac{\sigma_{red}}{\sigma_{ox} + \sigma_{red}} \quad (12)$$

$$\theta_{ox} = \frac{\sigma_{ox}}{\sigma_{ox} + \sigma_{red}} \quad (13)$$

The reaction rates of steps (10–11) are:

$$r_{CO_2} = k_{CO_2} \theta_{red}^{n_{CO_2}} \cdot Y_{CO_2}^{n_{CO_2}} \quad (14)$$

$$r_{H_2O} = k_{H_2O} \theta_{red}^{n_{H_2O}} \cdot Y_{H_2O}^{n_{H_2O}} \quad (15)$$

where θ_{red} is the reduced sites fraction, n_i are the reaction orders, Y_i are the reactants molar fractions, and k_i are the kinetic

TABLE 1 | Materials tested for the thermochemical splitting process, including nominal compositions (molar ratios), general formulas, and maximum oxygen evolutions (mmol/g).

Sample	Ce/Zr	M/(Ce + Zr)	K/(Ce + Zr)	General formula	$n_{O_2,max}$
K-CeZr	3	–	0.05	K _{0.05} Ce _{0.71} Zr _{0.24} O _{1.93}	1.16
K-Fe-CeZr	3	0.05	0.05	K _{0.045} Fe _{0.045} Ce _{0.68} Zr _{0.23} O _{1.91}	1.20
K-Cu-CeZr	3	0.05	0.05	K _{0.045} Cu _{0.045} Ce _{0.68} Zr _{0.23} O _{1.88}	1.28

constants which are evaluated as follows:

$$k_{CO_2} = k_{CO_2}^0 \exp\left(-\frac{E_{CO_2}}{RT}\right) \quad (16)$$

$$k_{H_2O} = k_{H_2O}^0 \exp\left(-\frac{E_{H_2O}}{RT}\right) \quad (17)$$

where E_i are the activation energies, and k_i^0 are the frequency factors.

The unsteady balance equations on reduced sites fraction for CO_2 splitting, H_2O splitting, and co-splitting are respectively:

$$\frac{d\theta_{red}}{dt} = -k_{CO_2}^0 \exp\left(-\frac{E_{CO_2}}{RT}\right) \theta_{red}^{n_{0_CO_2}} \cdot Y_{CO_2}^{n_{CO_2}} \quad (18)$$

$$\frac{d\theta_{red}}{dt} = -k_{H_2O}^0 \exp\left(-\frac{E_{H_2O}}{RT}\right) \theta_{red}^{n_{0_H_2O}} \cdot Y_{H_2O}^{n_{H_2O}} \quad (19)$$

$$\frac{d\theta_{red}}{dt} = -k_{CO_2}^0 \exp\left(-\frac{E_{CO_2}}{RT}\right) \theta_{red}^{n_{0_CO_2}} \cdot Y_{CO_2}^{n_{CO_2}} - k_{H_2O}^0 \exp\left(-\frac{E_{H_2O}}{RT}\right) \theta_{red}^{n_{0_H_2O}} \cdot Y_{H_2O}^{n_{H_2O}} \quad (20)$$

The unsteady balance equations on gaseous molar fractions are:

$$\frac{dY_{CO_2}}{dt} = \frac{Y_{CO_2}^{IN} - Y_{CO_2}}{\tau} - k_{CO_2} \theta_{red}^{n_{0_CO_2}} \cdot Y_{CO_2}^{n_{CO_2}} \quad (21)$$

$$\frac{dY_{H_2O}}{dt} = \frac{Y_{H_2O}^{IN} - Y_{H_2O}}{\tau} - k_{H_2O} \theta_{red}^{n_{0_H_2O}} \cdot Y_{H_2O}^{n_{H_2O}} \quad (22)$$

$$\frac{dY_{CO}}{dt} = \frac{Y_{CO}^{IN} - Y_{CO}}{\tau} - k_{CO_2} \theta_{red}^{n_{0_CO_2}} \cdot Y_{CO_2}^{n_{CO_2}} \quad (23)$$

$$\frac{dY_{H_2}}{dt} = \frac{Y_{H_2}^{IN} - Y_{H_2}}{\tau} - k_{H_2O} \theta_{red}^{n_{0_H_2O}} \cdot Y_{H_2O}^{n_{H_2O}} \quad (24)$$

where τ is the residence time equal to the experimental one.

The initial conditions are:

$$t = 0 \quad \theta_{red} = \theta^0 \quad (25)$$

$$t = 0 \quad Y_{CO_2} = 0.06 \quad (26)$$

$$t = 0 \quad Y_{H_2O} = 0.03 \text{ (H}_2\text{O splitting)}; 0.06 \text{ (co - splitting)} \quad (27)$$

$$t = 0 \quad Y_{CO} = 0 \quad (28)$$

$$t = 0 \quad Y_{H_2} = 0 \quad (29)$$

Differential equations were numerically solved using the Euler explicit method.

To analyze the fitting quality, the differences between the experimental data and the model were evaluated through the root mean square error (SRMSE), normalized for the maximum value of the curve of the flow test for each step:

$$SRMSE = \frac{1}{Y_{MAX}} \sqrt{\frac{1}{N} \sum_{i=1}^N (y_{exp}(i) - y_{mod}(i))^2} \quad (30)$$

Model and experimental curves were considered in good agreements for SRMSE values ≤ 0.045 .

RESULTS

Experimental Results

Previous research has reported on H_2/H_2O cycling, outlining that it can be used to define the splitting properties of materials (Landi, 2019). Results of thermogravimetric (TG) measurements (reduction under inert Ar atmosphere; oxidation under 40 vol.% CO_2/Ar) and H_2O splitting tests on H_2 -reduced samples were successfully compared (Al-Shankiti et al., 2013; Pappacena et al., 2016, 2017; Luciani et al., 2018).

Results by Landi (2019) showed that K-addition to bare ceria-zirconia and materials doped with transition metals (K-Fe-CeZr and K-Cu-CeZr) significantly enhance the evolved oxygen amount and lower the reduction onset temperature. These reduction profiles obtained for the co-splitting reaction are consistent with those reported by other studies (Landi, 2019) and will, therefore, not be further discussed.

Figure 1 (bottom) shows H_2 profiles measured in the H_2O splitting tests. The profiles refer to the stable performance obtained after the multiple reduction/oxidation cycle (Landi, 2019). One wide peak was detected over the K-Cu-CeZr sample, while two peaks were found over K-Fe-CeZr catalysts.

Potassium doped samples show faster oxidation kinetics than K-free materials (Landi, 2019). In particular, H_2 production occurs at very low temperature (peak temperature at $160^\circ C$ for K-Fe-CeZr and $200^\circ C$ for K-Cu-CeZr sample, respectively). Furthermore, the K-Fe-CeZr sample shows a second oxidation phenomenon at a higher temperature (at about $590^\circ C$).

Table 2 reports the amount of produced O_2 and H_2 , reduction degrees after each step (x_{red}), oxidation yields (α), and reduction yields (β) as obtained during H_2O splitting tests. Co-doped samples show higher oxygen and hydrogen production than the bare CeZr catalyst, as well as full re-oxidation (approximately 100%). Indeed, K-doping of M-doped ceria-zirconia ($M = Fe^{3+}$ and Cu^{2+}) can have limited effects on redox performance with no significant changes in the oxygen released (Fe-CeZr: K-free 847 $\mu mol/g$, K-doped 747 $\mu mol/g$; Cu-CeZr: K-free 576 $\mu mol/g$, K-doped 559 $\mu mol/g$) and produced hydrogen (Fe-CeZr: K-free 1,437 $\mu mol/g$, K-doped 1,458 $\mu mol/g$; Cu-CeZr: K-free 1,070 $\mu mol/g$, K-doped 1,237 $\mu mol/g$) (Landi, 2019).

The low temperature oxidation peak could be addressed to the contribution of surface and sub-surface layers and/or less ordered bulk structures to splitting reactions, while the high temperature peak could be related to the oxidation of bulk ceria-zirconia.

Figure 1 shows H_2 and CO concentration profiles as obtained in CO_2/H_2O co-splitting tests and separate H_2O and CO_2 splitting experiments over co-doped materials. **Figure 2** also shows the fuel amount produced over K-Fe-CeZr and K-Cu-CeZr catalysts.

K-Fe-CeZr sample shows two oxidation peaks independently from the oxidizing stream. In CO_2 splitting, the former peak ($450^\circ C$) occurs at a higher temperature than that found in H_2O

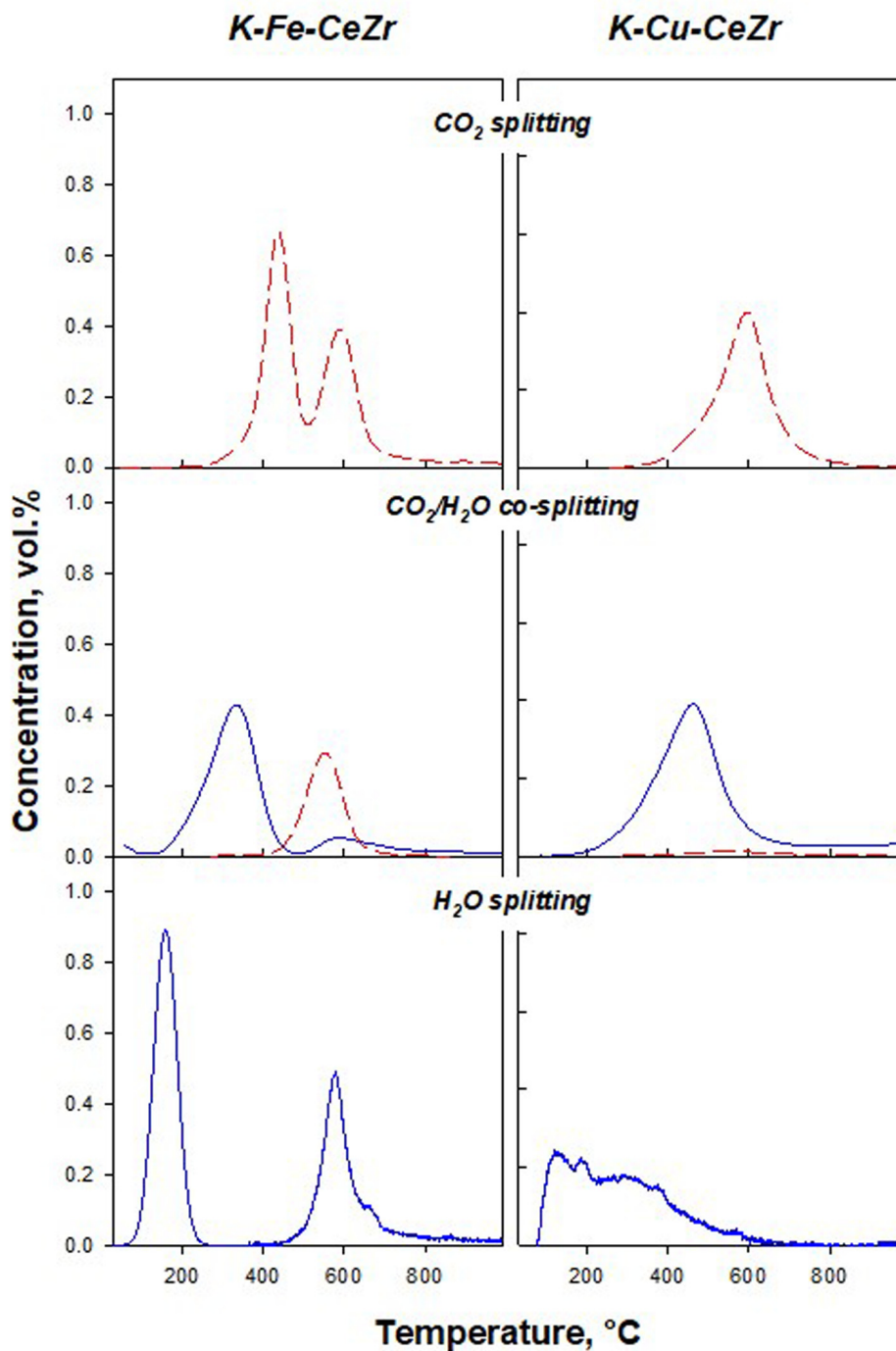


FIGURE 1 | H₂ (blue solid lines) and CO (red dashed lines) concentration profiles during splitting tests under different oxidizing streams on K-Fe-CeZr (**left**) and K-Cu-CeZr (**right**).

splitting. This result suggests that the H₂O splitting reaction is faster than the CO₂ reaction.

In H₂O/CO₂ co-splitting tests, the H₂O was reduced first. However, H₂O started reducing at 200°C reaching the peak at 330°C. This peak temperature is higher than bare H₂O splitting conditions. This behavior can be addressed to the CO₂ adsorption

on the surface, inhibiting H₂O adsorption and further reaction. Actually, in our previous papers, we showed that CO₂ desorption on ceria-based materials occurs at about 200°C (Di Benedetto et al., 2013; Barbato et al., 2016).

Moreover, CO₂ feed results in a lower produced H₂ amount (**Figure 2C**). The second oxidation phenomenon occurs

TABLE 2 | Amount (in $\mu\text{mol/g}$) of released oxygen (as O_2) and produced H_2 during H_2O splitting tests, reduction degrees after each step (x_{red}), oxidation yields (α), and reduction yields (β).

Sample	n_{O_2}	x_{red} (%)	β (%)	n_{H_2}	x_{red} (%)	α (%)
CeZr	450	56.3	206.4	509	34.6	56.5
K-CeZr	549	67.4	191.6	1380	7.7	125.7
K-Fe-CeZr	747	49.1	98.5	1458	-4.8	97.6
K-Cu-CeZr	559	81.0	105.2	1237	32.6	110.5

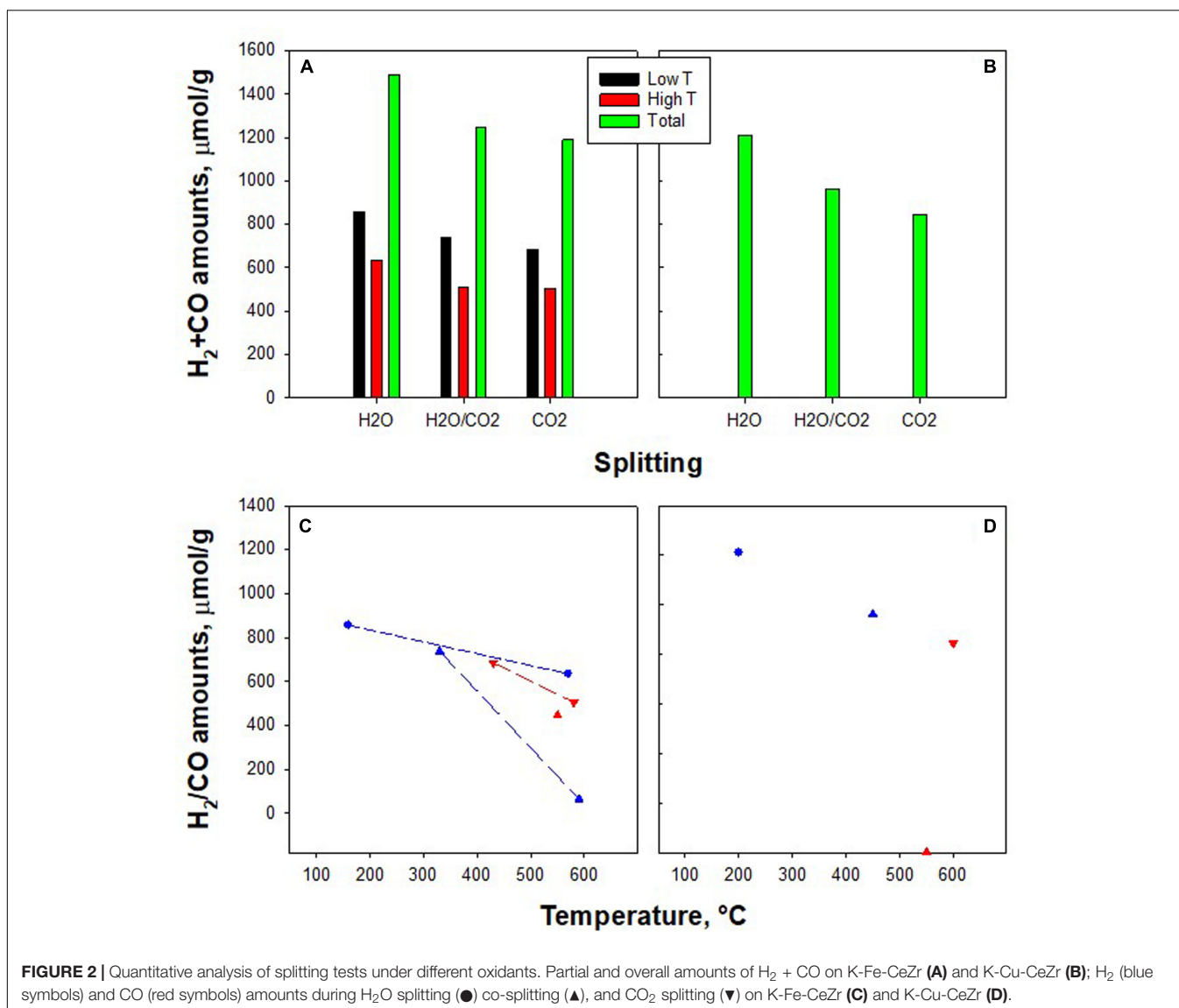
at the same temperature independently from the oxidizing stream (Figures 1, 2). As reported above, this peak is related to bulk oxidation. This reaction is controlled by the bulk-to-bulk oxygen diffusion and is thus not influenced by the chemical nature of the oxidant. However, during $\text{H}_2\text{O}/\text{CO}_2$ co-splitting only CO production is (unexpectedly)

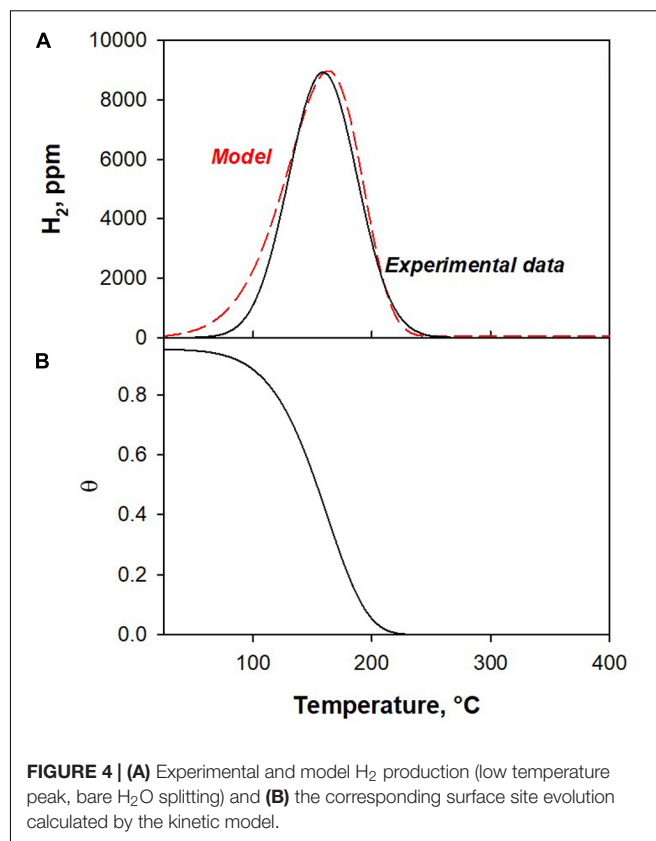
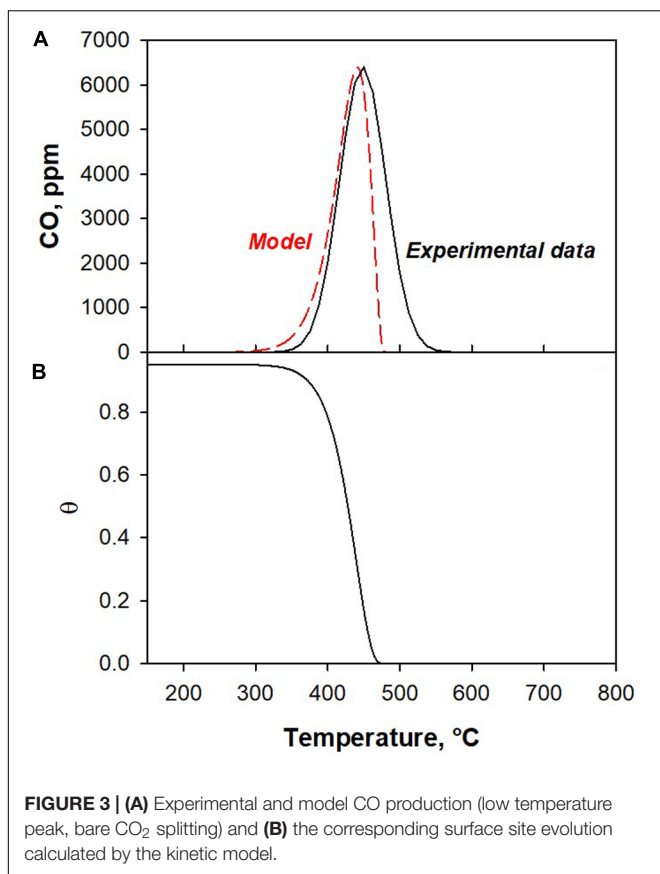
detected, suggesting a key role of gaseous molecules on the reaction pathway.

CO_2 splitting on K-Cu-CeZr (Figure 1) features one CO production peak at about 600°C , confirming lower activity toward CO_2 than the K-Fe-CeZr sample, which was also detected by TG analysis (Landi, 2019). In the $\text{H}_2\text{O}/\text{CO}_2$ co-splitting tests, the presence of CO_2 shifts H_2 production to higher temperatures (Figures 1, 2D) and reduces H_2 amounts (Figures 2B,D), as reported for the K-Fe-CeZr sample. Furthermore, CO production is negligible, probably because the material is fully oxidized at a temperature lower than that of CO_2 activation.

Kinetic Model of K-Fe-CeZr

The results of co-splitting tests (Figure 1) show that the H_2O splitting reaction is faster than CO_2 . However, at high temperatures, the H_2O splitting reaction is prevented and CO_2 splitting is favored. To understand the observed behavior, we





developed a kinetic model. As reported in section “Kinetic Model,” only the surface reactions have been modeled. The low temperature peaks of H₂O and CO₂ splitting tests were used as experimental data to calculate the kinetic parameters. **Figures 3, 4** show the experimental and model curves as obtained in H₂O and CO₂ splitting tests, respectively. The results reported in **Table 3**, show a low value of the SRMSE, suggesting that the fitting is good.

From the fitting results, we conclude that the activation energy of the CO₂ splitting reaction is higher than that of H₂O splitting. This enables the H₂O splitting reaction to proceed at a lower temperature than CO₂, as indicated by the results of this experiment.

We can also note that the H₂O oxidation reaction is in the first order for active sites concentration ($n_{\theta_H_2O} = 1$); whereas the CO₂ oxidation rate exhibits an order lower than 1 with respect to active sites concentration ($n_{\theta_CO_2} = 0.75$). This result suggests that CO₂ needs a lower number of nearby reduced sites, as expected due to the different structure of the CO₂ molecule.

To study the competition between the two reaction rates we defined the parameter R :

$$R = \frac{r_{CO_2}}{r_{H_2O}} \quad (31)$$

Figure 5 shows H₂O and CO₂ splitting reaction rates of on K-Fe-CeZr as calculated by the kinetic model as a function of the

TABLE 3 | Kinetic parameters of surface splitting reactions.

Parameter	r_{H_2O}	r_{CO_2}
E_{aj} (J/mol)	$4.61 \cdot 10^4$	$1.50 \cdot 10^5$
k_{0i}	$1.00 \cdot 10^5$	$3.50 \cdot 10^{10}$
θ^0	0.95	0.95
$n_{\theta i}$	1	0.75
$n_{\theta j}$	0	0
SRMSE	0.043	0.038

active sites concentration (θ), at different values of temperature. In these figures, θ values along the x-axis are decreasing.

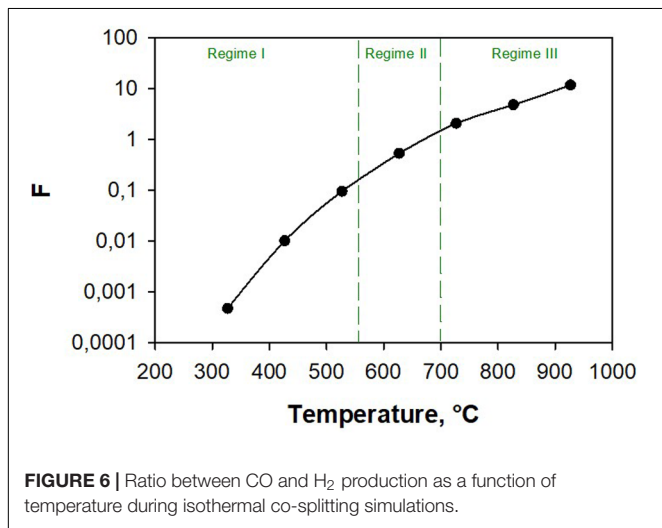
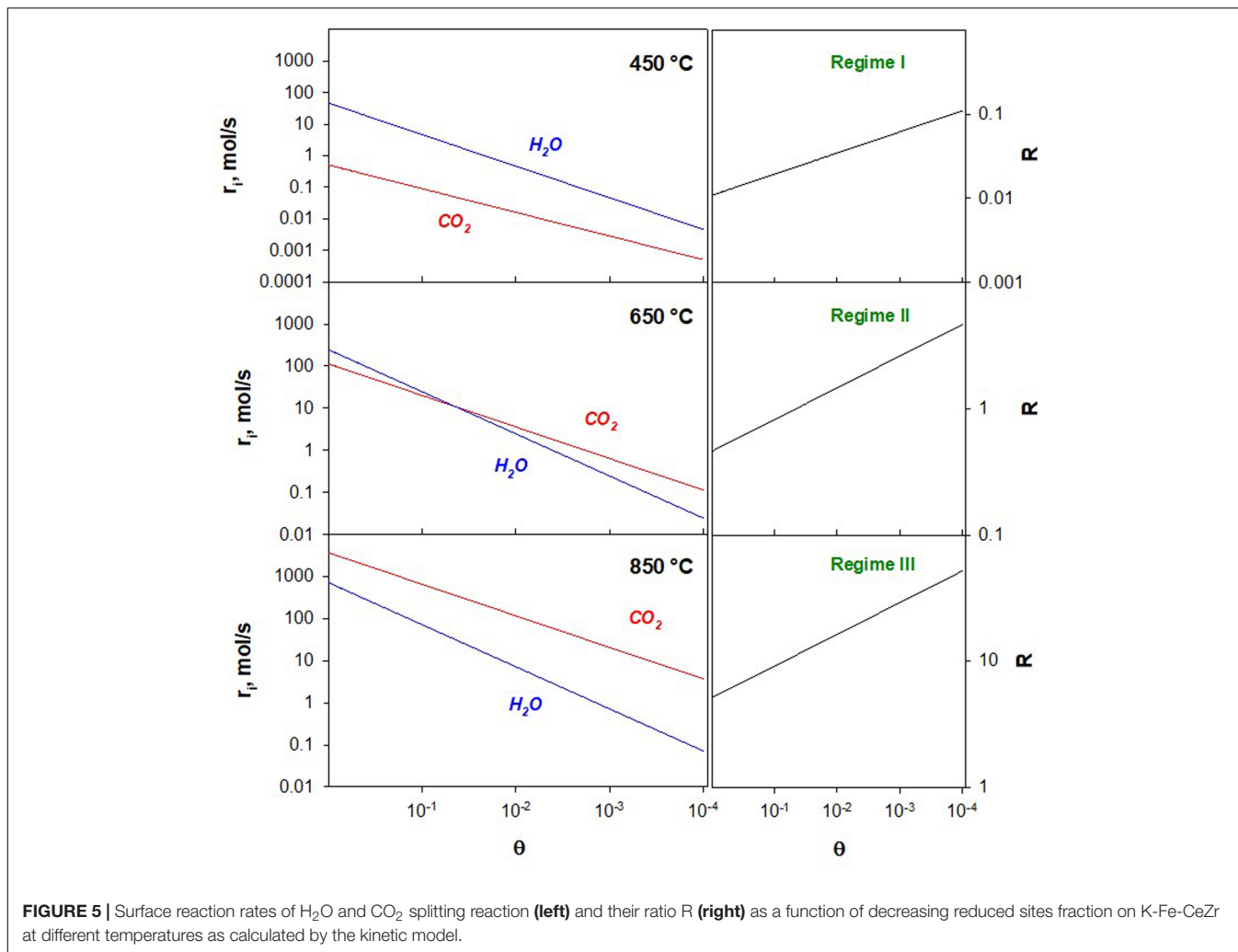
Three regimes can be identified:

Regime I- H₂O driven regime: @ $T \leq 560^\circ\text{C}$, the reaction rates do not intersect and $R < 1$ in the whole θ range. H₂ production prevails over CO production.

Regime II- mixed regime: @ $560 < T < 700^\circ\text{C}$, r_{CO_2} and r_{H_2O} intersect. At low θ values $R > 1$, at high θ values $R < 1$. Reaction rates are of the same order of magnitude, suggesting a co-production of carbon monoxide and hydrogen.

Regime III: CO₂ driven regime @ $T > 700^\circ\text{C}$ reaction rates do not intersect and $R > 1$ in the whole θ range. CO production prevails over H₂ production.

Isothermal simulations were performed to compute the amount of H₂ and CO produced as a function of temperature. **Figure 6** shows the ratio between CO and H₂ produced amounts



(F , Eq. 32) as a function of temperature.

$$F = \frac{n_{CO}}{n_{H_2}} \quad (32)$$

In this figure, the three regimes are also identified. It is worth noting that $F = 1$ at 670 °C and inversion occurs at higher temperatures.

From these results, we conclude that by changing the temperature, the content of H_2 and CO in the output current can be modulated.

CONCLUSION

In this work, ceria-zirconia was co-doped with transition metal (Cu^{2+} , Fe^{3+}) and potassium cations. We studied the co-doped ceria-zirconia to determine whether they act as catalysts for water and carbon dioxide co-splitting. All the investigated materials were able to convert separate feeds of CO_2 and H_2O into CO and H_2 , respectively. A single oxidation peak was detected on the K-Cu-CeZr catalyst, independently from the oxidant. Furthermore, the water splitting reaction rate appeared faster. Two oxidation peaks were detected on the K-Fe-CeZr catalyst for both the oxidants; the water reaction rate appeared faster at low temperature, while the high temperature peak seemed independent from the oxidant,

suggesting that the reaction rate is limited by the oxygen diffusion from the surface to the bulk.

Co-splitting tests were carried out as temperature programmed oxidations. On the K-Cu-CeZr catalyst, water reacted faster and a negligible CO production was detected. The H₂ production peak shifted to a higher temperature, probably due to CO₂ adsorption on the catalyst surface, thus blocking active sites. The K-Fe-CeZr catalyst behavior was more complex. Two oxidation peaks were detected at low and high temperatures. For the low temperature, only H₂ was produced in agreement with the faster H₂O splitting kinetics measured during the separated H₂O and CO₂ splitting. In contrast, almost 100% selectivity to CO₂ splitting was detected at high temperatures.

A kinetic model was developed to understand this behavior. This model revealed that the H₂O splitting reaction featured a higher reaction order in terms of sites fraction compared to CO₂. This suggests that H₂ production requires a larger number of adjacent reduced sites. By comparing the calculated surface reaction rates at different temperatures, three regimes were identified. At temperatures below 560°C H₂ production is faster than CO production independently from the surface reduced sites fraction; accordingly, isothermal co-splitting simulations showed a preeminent hydrogen production. At temperatures between 560 and 700°C, CO₂ and H₂O reaction rates are

comparable and the pre-eminence depends on both temperature and surface reduced sites fraction. In this temperature range, co-production of CO and H₂ occurs and their ratio can be tuned by an opportune choice of the co-splitting temperature. At temperatures higher than 700°C CO production is faster than H₂ production independently from the surface reduced sites fraction, accordingly, isothermal co-splitting simulations showed a preeminent carbon monoxide production.

DATA AVAILABILITY STATEMENT

The raw data supporting the conclusions of this article will be made available by the authors, without undue reservation.

AUTHOR CONTRIBUTIONS

GLa and GLu prepared the materials and performed the experiments. AD developed the model and performed the simulations. GLa, GLu, and AD contributed to the planning and interpretation of results, and the writing of the manuscript. All authors contributed to the article and approved the submitted version.

REFERENCES

- Abanades, S., and Le Gal, A. (2012). CO₂ splitting by thermo-chemical looping based on Zr xCe 1-xO₂ oxygen carriers for synthetic fuel generation. *Fuel* 102, 180–186. doi: 10.1016/j.fuel.2012.06.068
- Abanades, S., Legal, A., Cordier, A., Peraudeau, G., Flamant, G., and Julbe, A. (2010). Investigation of reactive cerium-based oxides for H₂ production by thermochemical two-step water-splitting. *J. Mater. Sci.* 45, 4163–4173. doi: 10.1007/s10853-010-4506-4504
- Agrafiotis, C., Roeb, M., and Sattler, C. (2015). A review on solar thermal syngas production via redox pair-based water/carbon dioxide splitting thermochemical cycles. *Renew. Sustain. Energy Rev.* 42, 254–285. doi: 10.1016/j.rser.2014.09.039
- Al-Shankiti, I., Al-Otaibi, F., Al-Salik, Y., and Idriss, H. (2013). Solar Thermal Hydrogen Production from Water over Modified CeO₂ Materials. *Top. Catal.* 56, 1129–1138. doi: 10.1007/s11244-013-0079-71
- Al-Shankiti, I., Ehrhart, B. D., and Weimer, A. W. (2017). Isothermal redox for H₂O and CO₂ splitting – A review and perspective. *Sol. Energy* 156, 21–29. doi: 10.1016/j.solener.2017.05.028
- Barbato, P. S., Colussi, S., Di Benedetto, A., Landi, G., Lisi, L., Llorca, J., et al. (2016). Origin of high activity and selectivity of CuO/CeO₂ catalysts prepared by solution combustion synthesis in CO-PROX reaction. *J. Phys. Chem. C* 120, 13039–13048. doi: 10.1021/acs.jpcc.6b02433
- Bhosale, R. R., and AlMomani, F. (2020). Hydrogen production via solar driven thermochemical cerium oxide – cerium sulfate water splitting cycle. *Int. J. Hydrogen Energy* 45, 10381–10390. doi: 10.1016/j.ijhydene.2019.05.159
- Bhosale, R. R., Kumar, A., Almomani, F., Ghosh, U., Al-Muhtaseb, S., Gupta, R., et al. (2016). Assessment of CexZryHfzO2 based oxides as potential solar thermochemical CO₂ splitting materials. *Ceram. Int.* 42, 9354–9362. doi: 10.1016/j.ceramint.2016.02.100
- Bhosale, R. R., Takalkar, G., Sutar, P., Kumar, A., AlMomani, F., and Khraisheh, M. (2019). A decade of ceria based solar thermochemical H₂O/CO₂ splitting cycle. *Int. J. Hydrogen Energy* 44, 34–60. doi: 10.1016/j.ijhydene.2018.04.080
- Bhosale, R. R., and Takalkar, G. D. (2018). Nanostructured co-precipitated Ce_{0.9}Ln_{0.1}O₂ (Ln = La, Pr, Sm, Nd, Gd, Tb, Dy, or Er) for thermochemical conversion of CO₂. *Ceram. Int.* 44, 16688–16697. doi: 10.1016/j.ceramint.2018.06.096
- Call, F., Roeb, M., Schmücker, M., Bru, H., Curulla-Ferre, D., Sattler, C., et al. (2013). Thermogravimetric analysis of Zirconia-Doped Ceria for thermochemical production of solar fuel. *Am. J. Anal. Chem.* 04, 37–45. doi: 10.4236/ajac.2013.410A1005
- Charvin, P., Abanades, S., Beche, E., Lemont, F., and Flamant, G. (2009). Hydrogen production from mixed cerium oxides via three-step water-splitting cycles. *Solid State Ionics* 180, 1003–1010. doi: 10.1016/j.ssi.2009.03.015
- Chen, Y., Zhu, X., Li, K., Wei, Y., Zheng, Y., and Wang, H. (2019). Chemical Looping Co-splitting of H₂O–CO₂ for Efficient Generation of Syngas. *ACS Sustain. Chem. Eng.* 7, 15452–15462. doi: 10.1021/acssuschemeng.9b02996
- Cho, H. S., Kodama, T., Gokon, N., Kim, J. K., Lee, S. N., and Kang, Y. H. (2017). “Development and experimental study for hydrogen production from the thermochemical two-step water splitting cycles with a CeO₂ coated new foam device design using solar furnace system,” in *Proceedings of the AIP Conference*, (College Park, MD: AIP), 100003. doi: 10.1063/1.4984460
- Chuayboon, S., and Abanades, S. (2020). An overview of solar decarbonization processes, reacting oxide materials, and thermochemical reactors for hydrogen and syngas production. *Int. J. Hydrogen Energy* 45, 25783–25810. doi: 10.1016/j.ijhydene.2020.04.098
- Cooper, T., Scheffe, J. R., Galvez, M. E., Jacot, R., Patzke, G., and Steinfeld, A. (2015). Lanthanum Manganite Perovskites with Ca/Sr A-site and Al B-site doping as effective oxygen exchange materials for solar thermochemical fuel production. *Energy Technol.* 3, 1130–1142. doi: 10.1002/ente.201500226
- Costa Oliveira, F. A., Barreiros, M. A., Abanades, S., Caetano, A. P. F., Novais, R. M., and Pullar, R. C. (2018). Solar thermochemical CO₂ splitting using cork-templated ceria ecoceramics. *J. CO₂ Util.* 26, 552–563. doi: 10.1016/j.jcou.2018.06.015
- Costa Oliveira, F. A., Barreiros, M. A., Haeussler, A., Caetano, A. P. F., Mouquinho, A. I., Oliveira e Silva, P. M., et al. (2020). High performance cork-templated ceria for solar thermochemical hydrogen production via two-step water-splitting cycles. *Sustain. Energy Fuels* 4, 3077–3089. doi: 10.1039/d0se00318b
- de la Calle, A., and Bayon, A. (2019). Annual performance of a thermochemical solar syngas production plant based on non-stoichiometric CeO₂. *Int. J. Hydrogen Energy* 44, 1409–1424. doi: 10.1016/j.ijhydene.2018.11.076

- Di Benedetto, A., Landi, G., Lisi, L., and Russo, G. (2013). Role of CO₂ on CO preferential oxidation over CuO/CeO₂ catalyst. *Appl. Catal. B Environ.* 142–143, 169–177. doi: 10.1016/j.apcatb.2013.05.001
- Falter, C., and Pitz-Paal, R. (2018). Energy analysis of solar thermochemical fuel production pathway with a focus on waste heat recuperation and vacuum generation. *Sol. Energy* 176, 230–240. doi: 10.1016/j.solener.2018.10.042
- Furler, P., Scheffe, J. R., and Steinfeld, A. (2012). Syngas production by simultaneous splitting of H₂O and CO₂ via ceria redox reactions in a high-temperature solar reactor. *Energy Environ. Sci.* 5, 6098–6103. doi: 10.1039/c1ee02620h
- Gokon, N., Sagawa, S., and Kodama, T. (2013). Comparative study of activity of cerium oxide at thermal reduction temperatures of 1300–1550 C for solar thermochemical two-step water-splitting cycle. *Int. J. Hydrogen Energy* 38, 14402–14414. doi: 10.1016/j.ijhydene.2013.08.108
- Gokon, N., Suda, T., and Kodama, T. (2015a). Oxygen and hydrogen productivities and repeatable reactivity of 30-mol% Fe-, Co-, Ni-, Mn-doped CeO_{2-δ} for thermochemical two-step water-splitting cycle. *Energy* 90, 1280–1289. doi: 10.1016/j.energy.2015.06.085
- Gokon, N., Suda, T., and Kodama, T. (2015b). Thermochemical reactivity of 5–15mol% Fe, Co, Ni, Mn-doped cerium oxides in two-step water-splitting cycle for solar hydrogen production. *Thermochim. Acta* 617, 179–190. doi: 10.1016/j.tca.2015.08.036
- Haeussler, A., Abanades, S., Julbe, A., Jouannaux, J., Drobek, M., Ayril, A., et al. (2020). Remarkable performance of microstructured ceria foams for thermochemical splitting of H₂O and CO₂ in a novel high-temperature solar reactor. *Chem. Eng. Res. Des.* 156, 311–323. doi: 10.1016/j.cherd.2020.02.008
- Hao, Y., Jin, J., and Jin, H. (2020). Thermodynamic analysis of isothermal CO₂ splitting and CO₂-H₂O co-splitting for solar fuel production. *Appl. Therm. Eng.* 166:113600. doi: 10.1016/j.applthermaleng.2019.04.010
- Jacot, R., Moré, R., Michalsky, R., Steinfeld, A., and Patzke, G. R. (2017). Trends in the phase stability and thermochemical oxygen exchange of ceria doped with potentially tetravalent metals. *J. Mater. Chem. A* 5, 19901–19913. doi: 10.1039/C7TA04063F
- Jarrett, C., Chueh, W., Yuan, C., Kawajiri, Y., Sandhage, K. H., and Henry, A. (2016). Critical limitations on the efficiency of two-step thermochemical cycles. *Sol. Energy* 123, 57–73. doi: 10.1016/j.solener.2015.09.036
- Kaneko, H., Taku, S., and Tamaura, Y. (2011). Reduction reactivity of CeO₂-ZrO₂ oxide under high O₂ partial pressure in two-step water splitting process. *Sol. Energy* 85, 2321–2330. doi: 10.1016/j.solener.2011.06.019
- Kang, M., Zhang, J., Wang, C., Wang, F., Zhao, N., Xiao, F., et al. (2013). CO₂ splitting via two step thermochemical reactions over doped ceria/zirconia solid solutions. *RSC Adv.* 3, 18878–18885. doi: 10.1039/C3RA43742F
- Landi, G. (2019). “Improving thermochemical splitting performance of ceria based materials: novel preparation routes, doping and co-doping,” in *International Conference on Nanoscience and Materials World (NSMW 2019)* Barcelona, Spain. Available online at: <https://www.coalesceresearchgroup.com/conferences/nanoscience>
- Le Gal, A., and Abanades, S. (2011). Catalytic investigation of ceria-zirconia solid solutions for solar hydrogen production. *Int. J. Hydrogen Energy* 36, 4739–4748. doi: 10.1016/j.ijhydene.2011.01.078
- Le Gal, A., and Abanades, S. (2012). Dopant incorporation in ceria for enhanced water-splitting activity during solar thermochemical hydrogen generation. *J. Phys. Chem. C* 116, 13516–13523. doi: 10.1021/jp302146c
- Le Gal, A., Abanades, S., Bion, N., Le Mercier, T., and Harlé, V. (2013). Reactivity of doped ceria-based mixed oxides for solar thermochemical hydrogen generation via two-step water-splitting cycles. *Energy Fuels* 27, 6068–6078. doi: 10.1021/ef4014373
- Lin, F., Samson, V. A., Wismer, A. O., Grolmund, D., Alxneit, I., and Wokaun, A. (2016). Zn-modified ceria as a redox material for thermochemical H₂O and CO₂ splitting: effect of a secondary ZnO phase on its thermochemical activity. *CrystEngComm* 18, 2559–2569. doi: 10.1039/C6CE00430J
- Lorentzou, S., Dimitrakis, D., Zygogianni, A., Karagiannakis, G., and Konstandopoulos, A. G. (2017). Thermochemical H₂O and CO₂ splitting redox cycles in a NiFe₂O₄ structured redox reactor: design, development and experiments in a high flux solar simulator. *Sol. Energy* 155, 1462–1481. doi: 10.1016/j.solener.2017.07.001
- Lorentzou, S., Karagiannakis, G., Pagkoura, C., Zygogianni, A., and Konstandopoulos, A. G. (2014). Thermochemical CO₂ and CO₂/H₂O splitting over NiFe₂O₄ for solar fuels synthesis. *Energy Procedia* 47, 1999–2008. doi: 10.1016/j.egypro.2014.03.212
- Luciani, G., Landi, G., Aronne, A., and Di Benedetto, A. (2018). Partial substitution of B cation in La_{0.6}Sr_{0.4}MnO₃perovskites: a promising strategy to improve the redox properties useful for solar thermochemical water and carbon dioxide splitting. *Sol. Energy* 171, 1–7. doi: 10.1016/j.solener.2018.06.058
- Luciani, G., Landi, G., Imparato, C., Vitiello, G., Deorsola, F. A., Di Benedetto, A., et al. (2019). Improvement of splitting performance of Ce_{0.75}Zr_{0.25}O₂ material: tuning bulk and surface properties by hydrothermal synthesis. *Int. J. Hydrogen Energy* 44, 17565–17577. doi: 10.1016/j.ijhydene.2019.05.021
- Mao, Y., Gao, Y., Dong, W., Wu, H., Song, Z., Zhao, X., et al. (2020). Hydrogen production via a two-step water splitting thermochemical cycle based on metal oxide – A review. *Appl. Energy* 267:114860. doi: 10.1016/j.apenergy.2020.114860
- Mostrou, S., Büchel, R., Pratsinis, S. E., and van Bokhoven, J. A. (2017). Improving the ceria-mediated water and carbon dioxide splitting through the addition of chromium. *Appl. Catal. A Gen.* 537, 40–49. doi: 10.1016/j.apcata.2017.03.001
- Muhich, C., and Steinfeld, A. (2017). Principles of doping ceria for the solar thermochemical redox splitting of H₂O and CO₂. *J. Mater. Chem. A* 5, 15578–15590. doi: 10.1039/C7TA04000H
- Muhich, C. L., Ehrhart, B. D., Al-Shankiti, I., Ward, B. J., Musgrave, C. B., and Weimer, A. W. (2016). A review and perspective of efficient hydrogen generation via solar thermal water splitting. *Wiley Interdiscip. Rev. Energy Environ.* 5, 261–287. doi: 10.1002/wene.174
- Naghavi, S. S., He, J., and Wolverson, C. (2020). CeTi₂O₆ - A Promising Oxide for Solar Thermochemical Hydrogen Production. *ACS Appl. Mater. Interfaces* 12, 21521–21527. doi: 10.1021/acsami.0c01083
- Nguyen, V. N., and Blum, L. (2015). Syngas and Synfuels from H₂O and CO₂: current status. *Chemie Ing. Tech.* 87, 354–375. doi: 10.1002/cite.201400090
- Pappacena, A., Boaro, M., Armelao, L., Llorca, J., and Trovarelli, A. (2016). Water splitting reaction on Ce_{0.15}Zr_{0.85}O₂ driven by surface heterogeneity. *Catal. Sci. Technol.* 6, 1–9. doi: 10.1039/C5CY01337B
- Pappacena, A., Rancan, M., Armelao, L., Llorca, J., Ge, W., Ye, B., et al. (2017). New Insights into the Dynamics That Control the Activity of Ceria-Zirconia Solid Solutions in Thermochemical Water Splitting Cycles. *J. Phys. Chem. C* 121, 17746–17755. doi: 10.1021/acs.jpcc.7b06043
- Petkovich, N. D., Rudisill, S. G., Venstrom, L. J., Boman, D. B., Davidson, J. H., and Stein, A. (2011). Control of heterogeneity in nanostructured Ce_{1-x}Zr_xO₂ Binary oxides for enhanced thermal stability and water splitting activity. *J. Phys. Chem. C* 115, 21022–21033. doi: 10.1021/jp2071315
- Portarapillo, M., Aronne, A., Di Benedetto, A., Imparato, C., Landi, G., and Luciani, G. (2019). Syngas production through H₂O/CO₂ thermochemical splitting. *Chem. Eng. Trans.* 74, 43–48. doi: 10.3303/CET1974008
- Rao, C. N. R., and Dey, S. (2015). Generation of H₂ and CO by solar thermochemical splitting of H₂O and CO₂ by employing metal oxides. *J. Solid State Chem.* 242, 107–115. doi: 10.1016/j.jssc.2015.12.018
- Takacs, M., Scheffe, J. R., and Steinfeld, A. (2015). Oxygen nonstoichiometry and thermodynamic characterization of Zr doped ceria in the 1573–1773 K temperature range. *Phys. Chem. Chem. Phys.* 17, 7813–7822. doi: 10.1039/C4CP04916K
- Takalkar, G., Bhosale, R. R., and AlMomani, F. (2019). Thermochemical splitting of CO₂ using Co-precipitation synthesized Ce_{0.75}Zr_{0.25}M_{0.05}O_{2-δ} (M = Cr, Mn, Fe, Co, Ni, Zn) materials. *Fuel* 256:115834. doi: 10.1016/j.fuel.2019.115834
- Takalkar, G., Bhosale, R. R., AlMomani, F., and Rashid, S. (2020a). Co-precipitation synthesized nanostructured Ce_{0.9}Ln_{0.05}Ag_{0.05}O_{2-δ} materials for solar thermochemical conversion of CO₂ into fuels. *J. Mater. Sci.* 55, 9748–9761. doi: 10.1007/s10853-020-04567-w
- Takalkar, G., Bhosale, R. R., Rashid, S., AlMomani, F., Shakoor, R. A., and Al Ashraf, A. (2020b). Application of Li-, Mg-, Ba-, Sr-, Ca-, and Sn-doped ceria for solar-driven thermochemical conversion of carbon dioxide. *J. Mater. Sci.* 55, 11797–11807. doi: 10.1007/s10853-020-04875-4871
- Takalkar, G. D., Bhosale, R. R., Kumar, A., AlMomani, F., Khraisheh, M., Shakoor, R. A., et al. (2018). Transition metal doped ceria for solar thermochemical fuel production. *Sol. Energy* 172, 204–211. doi: 10.1016/j.solener.2018.03.022
- Tou, M., Jin, J., Hao, Y., Steinfeld, A., and Michalsky, R. (2019). Solar-driven co-thermolysis of CO₂ and H₂O promoted by: in situ oxygen removal across

- a non-stoichiometric ceria membrane. *React. Chem. Eng.* 4, 1431–1438. doi: 10.1039/c8re00218e
- Zhao, B., Huang, C., Ran, R., Wu, X., and Weng, D. (2016). Two-step thermochemical looping using modified ceria-based materials for splitting CO₂. *J. Mater. Sci.* 51, 2299–2306. doi: 10.1007/s10853-015-9534-9537
- Zhou, Y., Deng, J., Lan, L., Wang, J., Yuan, S., Gong, M., et al. (2017). Remarkably promoted low-temperature reducibility and thermal stability of CeO₂-ZrO₂-La₂O₃-Nd₂O₃ by a urea-assisted low-temperature (90°C) hydrothermal procedure. *J. Mater. Sci.* 52, 5894–5907. doi: 10.1007/s10853-017-0825-z

Conflict of Interest: The authors declare that the research was conducted in the absence of any commercial or financial relationships that could be construed as a potential conflict of interest.

Copyright © 2020 Luciani, Landi and Di Benedetto. This is an open-access article distributed under the terms of the Creative Commons Attribution License (CC BY). The use, distribution or reproduction in other forums is permitted, provided the original author(s) and the copyright owner(s) are credited and that the original publication in this journal is cited, in accordance with accepted academic practice. No use, distribution or reproduction is permitted which does not comply with these terms.